pFedBBN: A Personalized Federated Test-Time Adaptation with Balanced Batch Normalization for Class-Imbalanced Data

Anonymous authors
Paper under double-blind review

Abstract

Test-time adaptation (TTA) in federated learning (FL) is crucial for handling unseen data distributions across clients, particularly when faced with domain shifts and skewed class distributions. Class Imbalance (CI) remains a fundamental challenge in FL, where rare but critical classes are often severely underrepresented in individual client datasets. Although prior work has addressed CI during training through reliable aggregation and local class distribution alignment, these methods typically rely on access to labeled data or coordination among clients, and none address class unsupervised adaptation to dynamic domains or distribution shifts at inference time under federated CI constraints. Revealing the failure of state-of-the-art TTA in federated client adaptation in CI scenario, we propose **pFedBBN**, a personalized federated test-time adaptation framework that employs balanced batch normalization (BBN) during local client adaptation to mitigate prediction bias by treating all classes equally, while also enabling client collaboration guided by BBN similarity, ensuring that clients with similar balanced representations reinforce each other and that adaptation remains aligned with domain-specific characteristics. pFedBBN supports fully unsupervised local adaptation and introduces a class-aware model aggregation strategy that enables personalized inference without compromising privacy. It addresses both distribution shifts and class imbalance through balanced feature normalization and domain-aware collaboration, without requiring any labeled or raw data from clients. Extensive experiments across diverse baselines show that pFedBBN consistently enhances robustness and minority-class performance over state-of-the-art FL and TTA methods

1 Introduction

Federated Learning (FL) enables decentralized training across a network of clients, such as smartphones, hospitals, or IoT devices—without sharing raw data. This is critical in privacy-sensitive domains like mobile computing, healthcare, and smart environments McMahan et al. (2017); Chen et al. (2025); Noble et al. (2022); Liu et al. (2024). However, data in FL is often non-identically distributed (non-IID), evolves over time, and suffers from severe class imbalance, making reliable inference particularly challenging.

Test-Time Adaptation (TTA) aims to enhance generalization under distribution shifts by adapting models using unlabeled test inputs. It is necessary in dynamic environments where client data distributions continually change. However, adapting from unlabeled data can lead to error and catastrophic forgetting Niu et al. (2022), especially when adaptation occurs continuously in real-world settings.

In FL, TTA is even more challenging due to the presence of heterogeneous client domains and the absence of labeled test data. Further, class imbalance Xiao & Wang (2021); Wang et al. (2021b); Seol & Kim (2023) is a fundamental issue: dominant classes often overshadow rare but critical ones (e.g., emergency alerts or abnormal health readings), degrading model performance on minority classes.

Existing class imbalance mitigation techniques, such as resampling Khushi et al. (2021), data augmentation Duan et al. (2020), or cost-sensitive lossesSarkar et al. (2020); Khan et al. (2017) which

are ill-suited for FL. These methods assume access to raw data, which violates privacy, or fail when applied locally without coordination. FL-specific solutions often require proxy servers Huang et al. (2016), auxiliary models Wang et al. (2017), or data exchange, introducing overhead and compromising privacy. Then, a paper Wang et al. (2021b) proposed a federated learning approach to mitigate class imbalance by adjusting training dynamics using labeled data across clients. However, their method is designed for the training phase and does not address class imbalance in the test-time adaptation setting.

In TTA, the challenges compound. Without labels, correcting for both domain shifts and class imbalance becomes significantly harder. Batch Normalization (BN) statistics, commonly used in TTA, become biased You et al. (2021) due to dominant classes, resulting in degraded adaptation. Unsupervised adaptation exacerbates the problem, as both error accumulation and imbalanced normalization persist without the availability of ground truth. The recently proposed FedCTTA Rajib et al. (2025) addresses domain adaptation in Federated Test-Time Adaptation (TTA) through a collaborative continual adaptation strategy. However, it does not explicitly tackle the challenge of class imbalance, which remains an open problem in TTA for FL settings.

To address these issues, we propose **pFedBBN**, the first framework that tackles class imbalance in federated test-time adaptation. Our method enables clients to adapt models using local unlabeled data while leveraging domain-similar peers for personalized model aggregation. A new *Class-Wise Adaptive Normalization (CWAN)* module tracks per-class feature statistics with pseudo-labels and interpolates them with batch-level statistics to mitigate imbalance. Further, a *confidence-filtered self-distillation* approach selectively updates the model using pseudo-labeled data. Only the BN affine parameters are updated to preserve generalization. Clients then share BN statistics to infer domain similarity and receive personalized models via similarity-aware aggregation, all under strict privacy constraints.

In summary, the key contributions of this work are:

- We propose **pFedBBN**, the first framework specifically designed to address *class imbalance* in federated test-time adaptation, where clients adapt models using unlabeled, locally available test data under domain and class distribution shifts.
- We introduce a **Class-Wise Adaptive Normalization (CWAN)** module that maintains *per-class feature statistics* using pseudo-labels. By interpolating these with batch-level statistics, CWAN mitigates the bias introduced by dominant classes during adaptation without accessing ground-truth labels.
- To reduce the impact of noisy pseudo-labels, we apply a **confidence-based filtering** mechanism that selectively updates the model using only high-confidence pseudo-labeled samples via self-distillation, effectively minimizing error accumulation and catastrophic forgetting.
- We conduct comprehensive experiments on non-IID, class-imbalanced, and domain-shifted settings, demonstrating the effectiveness of pFedBBN over state-of-the-art FL and TTA baselines.

2 Related Work

Federated Learning. Federated learning (FL) McMahan et al. (2017) enables collaborative model training across decentralized clients without directly sharing raw data, which is essential in privacy-sensitive domains such as healthcare, mobile computing, and IoT. However, challenges such as non-IID data distributions, class imbalance, and domain heterogeneity remain fundamental obstacles. Several works have explored methods to improve robustness under such settings, including communication-efficient optimization Chen et al. (2025), privacy-preserving learning with differential privacy Noble et al. (2022), and adaptive personalization Liu et al. (2024).

Class Imbalance in FL. Class imbalance is a critical challenge in FL, as dominant classes can overshadow rare yet important ones. Traditional solutions include resampling Khushi et al. (2021), data augmentation Duan et al. (2020), and cost-sensitive losses Sarkar et al. (2020); Khan et al. (2017). However, these methods typically assume access to centralized raw data, making them unsuitable for federated settings. FL-specific approaches have been proposed, including the use of proxy servers Huang et al. (2016), auxiliary models Wang et al. (2017), or data sharing among

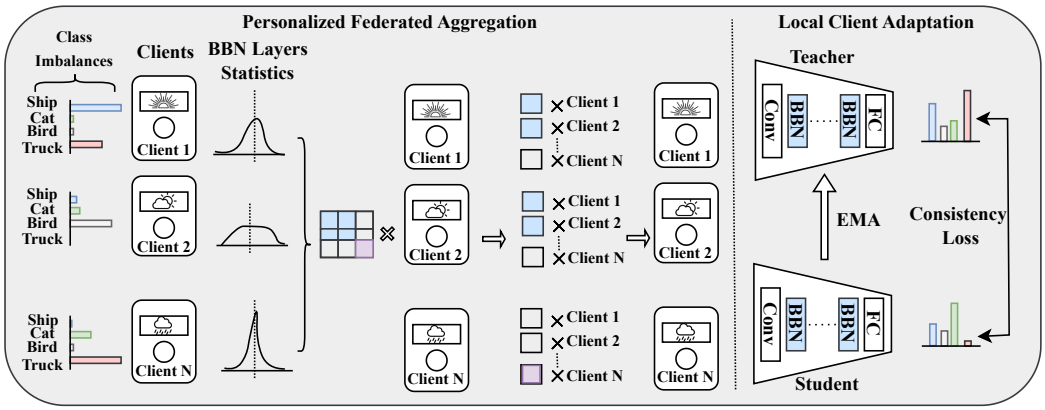

Figure 1: The overall framework of pFedBBN where each client performs unsupervised local adaptation using class-wise balanced batch normalization (BBN) and confidence-filtered distillation. Adapted batch normalization statistics are then used to compute client similarities, enabling personalized aggregation without sharing raw data.

clients. Yet, such methods raise privacy and communication concerns. More recently, Wang et al. Wang et al. (2021b) proposed a federated optimization method that adjusts training dynamics across clients to address imbalance. However, this work focuses on the training phase and does not extend to test-time adaptation.

Test-Time Adaptation. Test-time adaptation (TTA) methods aim to improve generalization under distribution shifts by adapting models using unlabeled test data. Recent work has shown the effectiveness of updating Batch Normalization (BN) statistics for adaptation You et al. (2021), although such methods often suffer from error accumulation and catastrophic forgetting in the absence of ground-truth supervision Niu et al. (2022). Moreover, BN statistics are particularly vulnerable to skewed class distributions, leading to biased adaptation under imbalance.

Federated Test-Time Adaptation. Federated TTA is even more challenging, since clients face heterogeneous domain shifts, non-IID distributions, and the absence of labels. The recently proposed FedCTTA Rajib et al. (2025) introduced a collaborative continual adaptation strategy that improves robustness under distribution shifts. However, it does not explicitly address the challenge of class imbalance, which remains an open problem in federated TTA.

In contrast, our work introduces **pFedBBN**, the first framework that explicitly tackles class imbalance in federated test-time adaptation. Our approach incorporates a class-wise adaptive normalization mechanism with pseudo-labeling, confidence-based self-distillation, and similarity-aware aggregation, enabling privacy-preserving adaptation under distribution and class imbalance shifts.

3 METHODOLOGY

In real-world FL, clients face non-stationary, heterogeneous data that diverges from the source model. To ensure robust, personalized inference, we propose a unified framework that enables local test-time adaptation on unlabeled data and collaboration with similar clients via distance-aware aggregation. Our method includes three components: unsupervised local adaptation using class-wise normalization and confidence distillation, similarity estimation via batch normalization statistics, and personalized aggregation based on domain alignment.

3.1 UNSUPERVISED LOCAL CLIENT ADAPTATION

In the absence of labeled data, each client must adapt to its own distribution shift using only the pretrained source model. Our client-side test-time adaptation framework comprises two core strategies:

Class-Wise Adaptive Normalization (CWAN) to address distributional drift and Confidence-Filtered Distillation to guide learning through self-supervision.

3.1.1 CLASS-WISE ADAPTIVE NORMALIZATION (CWAN)

Standard batch normalization relies on assumptions of stationary, class-balanced data, which break down in federated settings due to non-IID client distributions. To correct for this, we propose CWAN, which dynamically tracks per-class statistics at test time based on pseudo-labels assigned by the source model.

Let $\mathbf{z}_i \in \mathbb{R}^d$ be the feature vector input to the normalization layer for test input $\mathbf{x}_i$, with pseudo-label $\hat{c}_i \in \{1, \ldots, K\}$. For each class k, we maintain exponentially moving estimates of mean $\boldsymbol{\mu}_k^{(t)}$ and variance $\boldsymbol{\Sigma}_k^{(t)}$ at iteration t:

$$\boldsymbol{\mu}_k^{(t)} = (1 - \alpha) \cdot \boldsymbol{\mu}_k^{(t-1)} + \alpha \cdot \bar{\mathbf{z}}_k^{(t)} \tag{1}$$

$$\boldsymbol{\Sigma}_k^{(t)} = (1 - \alpha) \cdot \boldsymbol{\Sigma}_k^{(t-1)} + \alpha \cdot \widehat{\mathrm{Var}}_k^{(t)} \tag{2}$$

These are aggregated into global estimates across classes:

$$\boldsymbol{\mu}_{\text{global}}^{(t)} = \frac{1}{K} \sum_{k=1}^{K} \boldsymbol{\mu}_k^{(t)} \tag{3}$$

$$\boldsymbol{\Sigma}_{\text{global}}^{(t)} = \frac{1}{K} \sum_{k=1}^{K} \left(\boldsymbol{\Sigma}_k^{(t)} + (\boldsymbol{\mu}_k^{(t)} - \boldsymbol{\mu}_{\text{global}}^{(t)})^2 \right) \tag{4}$$

To manage pseudo-label noise or limited class representation, we interpolate per-class and batch-wise statistics via $\beta \in [0, 1]$:

$$\tilde{\boldsymbol{\mu}}_i^{(t)} = (1 - \beta) \cdot \boldsymbol{\mu}_{\hat{c}_i}^{(t)} + \beta \cdot \bar{\mathbf{z}}^{(t)} \tag{5}$$

$$\tilde{\boldsymbol{\Sigma}}_i^{(t)} = (1 - \beta) \cdot \boldsymbol{\Sigma}_{\hat{c}_i}^{(t)} + \beta \cdot \widehat{\mathrm{Var}}^{(t)} \tag{6}$$

The normalized feature is then computed as:

$$\hat{\mathbf{z}}_i = \frac{\mathbf{z}_i - \tilde{\boldsymbol{\mu}}_i^{(t)}}{\sqrt{\tilde{\boldsymbol{\Sigma}}_i^{(t)} + \epsilon}} \cdot \boldsymbol{\gamma} + \boldsymbol{\beta}$$

where $\boldsymbol{\gamma}, \boldsymbol{\beta}$ are the affine parameters, and ϵ is a stability constant.

3.1.2 CONFIDENCE-FILTERED DISTILLATION

To further refine local model behavior, we incorporate a self-supervised knowledge distillation mechanism. The source model $\mathcal{F}_s$ serves as a frozen teacher, and a student model $\mathcal{F}_t$ (initialized identically) is adapted locally using confident pseudo-labels.

For a test input $\mathbf{x}$ and its augmented variant $\tilde{\mathbf{x}}$, predictions from teacher and student are:

$$\mathbf{p}_t = \mathrm{softmax}(\mathcal{F}_s(\mathbf{x})), \quad \mathbf{p}_s = \mathrm{softmax}(\mathcal{F}_t(\tilde{\mathbf{x}}))$$

A confidence threshold δ filters uncertain samples via entropy:

$$H(\mathbf{p}_t) < \delta$$

Letting $\hat{y} = \arg\max \mathbf{p}_t$, the distillation loss becomes:

$$\mathcal{L}_{\text{distill}} = \frac{1}{B} \sum_{i=1}^{B} \mathbb{I}\left[H(\mathbf{p}_{t,i}) < \delta\right] \cdot \mathrm{CE}(\hat{y}_i, \mathbf{p}_{s,i}) \tag{7}$$

To preserve the model's generalization capability, only the affine parameters in the normalization layers of $\mathcal{F}_t$ are updated during adaptation.

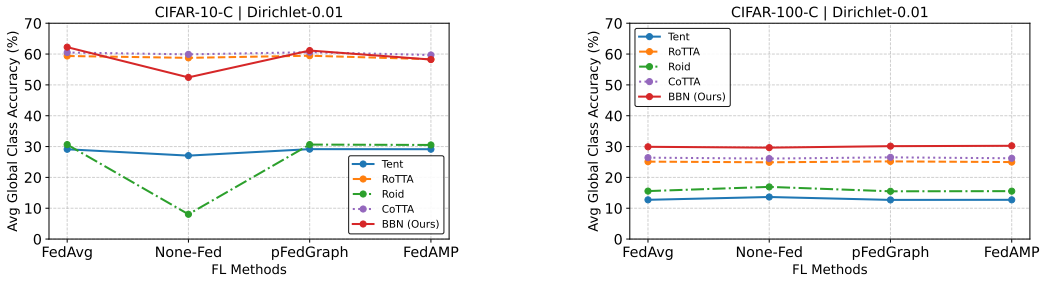

(a) CIFAR-10-C (b) CIFAR-100-C

Figure 2: Average global class accuracies (%) of different TTA methods

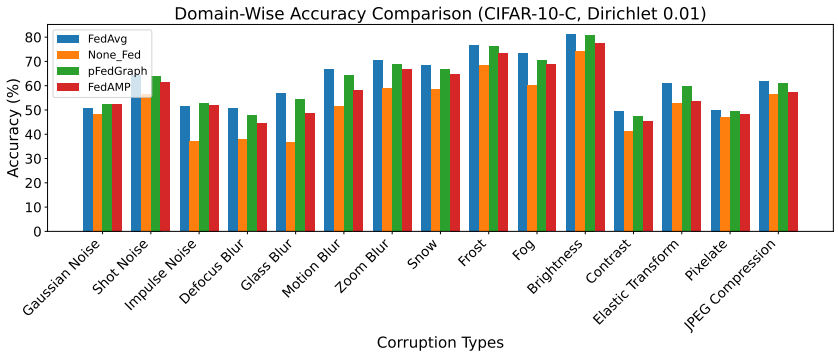

Figure 3: Domain-wise accuracy comparison of our method (Dirichlet $\alpha = 0.01$) across CIFAR-10-C corruptions.

3.2 Batch Normalization Statistics for Domain Similarity

Once local adaptation is complete, each client possesses a refined model whose batch normalization layers encode a statistical summary of the local feature distribution. These statistics form the basis for client similarity estimation used during aggregation.

Let $\mathcal{L}$ denote the set of BN layers, and for each client i and layer $\ell \in \mathcal{L}$, let $\boldsymbol{\mu}_\ell^{(i)}, \boldsymbol{\sigma}_\ell^{2(i)} \in \mathbb{R}^d$ be the flattened global mean and variance vectors, respectively. The pairwise distance between clients i and j is given by:

$$D_{ij} = \frac{1}{|\mathcal{L}|} \sum_{\ell \in \mathcal{L}} \frac{1}{2} \left(\|\boldsymbol{\mu}_\ell^{(i)} - \boldsymbol{\mu}_\ell^{(j)}\|_2 + \|\boldsymbol{\sigma}_\ell^{2(i)} - \boldsymbol{\sigma}_\ell^{2(j)}\|_2 \right) \tag{8}$$

This defines a symmetric distance matrix $D \in \mathbb{R}^{N \times N}$ across N clients.

3.3 Personalized Federated Aggregation

To prevent negative transfer from dissimilar domains, we propose a soft similarity-based aggregation strategy that personalizes the global model for each client based on domain closeness.

3.3.1 Similarity-Weighted Collaboration Matrix

We derive a row-stochastic similarity matrix $W \in \mathbb{R}^{N \times N}$ from D using a temperature-controlled softmax:

$$W_{ij} = \begin{cases} \frac{\exp(-D_{ij}/\tau)}{\sum_{k \neq i} \exp(-D_{ik}/\tau)} \cdot (1 - \omega_i), & j \neq i \\ \omega_i, & j = i \end{cases} \tag{9}$$

Table 1: Comparison of federated learning (FL) methods with different test-time adaptation (TTA) techniques on CIFAR-10-C and CIFAR-100-C benchmark datasets with 10 clients. Results are reported for both IID and non-IID settings (Dirichlet partitioning with $\alpha \in 0.005, 0.01, 0.1$). Gray-highlighted rows correspond to our proposed BBN module, while the last row (pFedBBN) represents our full framework.

Fed Method	**TTA Method**	**CIFAR-10-C**				**CIFAR-100-C**			
		IID	**Non-IID**			**IID**	**Non-IID**		
			α=0.005	α=0.01	α=0.1		α=0.005	α=0.01	α=0.1
Any	Source	56.51	58.28	58.58	56.11	54.28	54.58	57.14	53.03
None	Tent	81.08	23.99	24.98	31.23	68.59	6.84	9.41	28.19
	CoTTA	81.78	21.13	23.42	31.06	66.24	6.01	10.88	28.94
	ROID	81.44	14.60	15.95	26.20	69.41	7.46	11.84	38.38
	RoTTA	66.63	30.64	32.73	51.06	50.60	15.03	28.31	44.61
	BBN	72.32	56.88	52.33	70.53	59.32	64.07	72.31	66.21
FedAvg	Tent	81.19	21.51	22.47	29.42	68.13	5.06	7.82	25.27
	CoTTA	81.61	19.92	21.11	28.74	65.94	6.08	9.32	32.53
	ROID	81.85	22.93	23.96	32.15	69.06	6.85	10.97	37.01
	RoTTA	64.16	64.54	64.34	64.68	49.15	49.46	55.00	49.07
	BBN	72.61	68.47	69.04	74.05	60.08	67.49	71.30	63.03
FedProx	Tent	81.20	21.52	22.47	29.42	68.13	5.06	7.82	25.27
	CoTTA	81.59	19.92	23.69	30.98	65.95	6.07	10.85	29.19
	ROID	81.81	20.87	24.02	31.77	69.30	6.86	10.69	37.01
	RoTTA	67.31	39.39	64.41	64.69	49.82	22.66	55.04	48.98
FedAvgM	Tent	81.30	21.45	22.37	29.38	67.52	5.05	7.82	25.39
	CoTTA	81.95	19.88	21.45	28.50	66.12	6.42	9.01	32.75
	ROID	81.87	23.07	24.09	32.35	68.81	6.87	11.11	37.04
	RoTTA	38.88	39.73	39.42	37.86	17.95	34.36	38.54	21.56
pfedGraph	Tent	81.19	21.52	22.49	29.98	68.11	5.12	7.83	25.04
	CoTTA	81.64	19.94	22.34	29.01	65.99	6.08	10.88	29.03
	ROID	81.84	22.99	23.96	32.34	69.07	5.88	10.96	36.91
	RoTTA	64.87	63.75	64.43	63.98	49.51	52.99	54.88	54.63
	BBN	72.73	69.37	66.89	73.54	60.14	67.29	72.61	63.71
FedAmp	Tent	81.19	20.65	22.49	28.28	68.15	5.09	7.85	25.30
	CoTTA	81.61	20.19	22.93	30.21	65.95	6.07	10.23	28.71
	ROID	81.83	21.11	23.82	33.11	69.11	6.88	11.21	36.88
	RoTTA	65.91	63.87	62.85	63.16	50.27	46.82	53.91	49.35
	BBN	72.36	63.16	61.36	72.53	59.52	69.88	72.62	63.29
pFedBBN	BBN	70.11	72.41	71.96	68.53	65.29	71.96	73.88	64.29

with self-weight ω_i defined as:

$$\omega_i = \frac{1}{1 + \sum_{k \neq i} \exp(-D_{ik}/\tau)} \tag{10}$$

This ensures each client gives more weight to peers with similar BN statistics while preserving a degree of self-reliance.

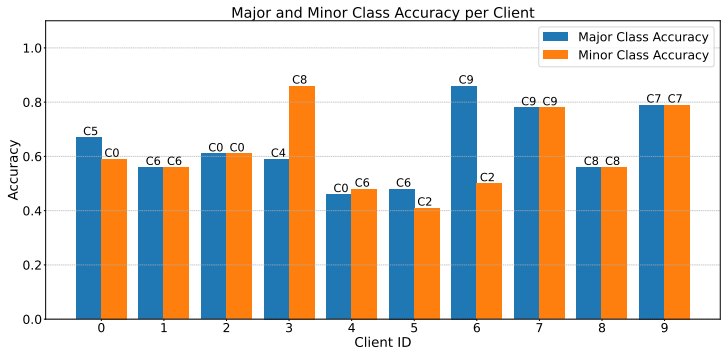

Figure 4: Major and Minor Class Accuracy per Client.

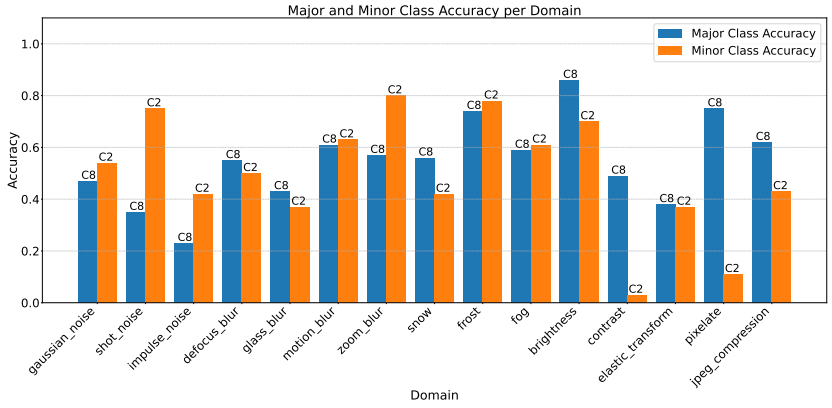

Figure 5: Major and minor class accuracy per domain.

3.3.2 Aggregated Personalized Model

Each client receives a personalized model computed as:

$$\theta_{\text{agg}}^{(i)} = \sum_{j=1}^{N} W_{ij} \cdot \theta^{(j)} \tag{11}$$

This model is then used for continued inference or further local adaptation on client i's stream.

3.4 Privacy Concerns

The entire process integrates local adaptation and collaborative learning into a coherent pipeline. Each client adapts its BN statistics using CWAN and updates normalization affine parameters via filtered distillation. Adapted BN statistics are shared with the server to compute inter-client distances. The server constructs a personalized model for each client using similarity-weighted aggregation. Clients receive their aggregated models and continue local operations. The key insight of this approach is that batch normalization statistics offer a compact and domain-aware signature of the client's data distribution. By using these adapted statistics to guide server-side aggregation, the method naturally clusters clients with similar domain properties, even in the absence of explicit metadata or labels.

This personalized aggregation scheme is privacy-preserving, as only internal statistics (not raw data or features) are used. It is unsupervised, relying solely on pseudo-label-driven adaptation. It is scalable, with communication cost comparable to traditional federated averaging. The combination of locally adapted BN statistics and global distance-aware aggregation ensures both domain alignment and robustness to heterogeneity, improving generalization in federated test-time environments.

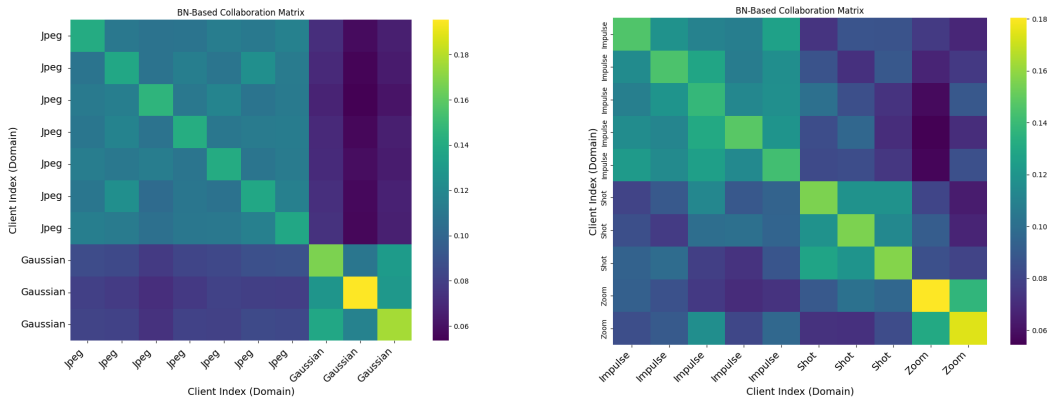

(a) Collaboration Matrix Round 40

(b) Collaboration Matrix Round 75

Figure 6: Collaboration Matrix of our pFedBBN which indicates which client give more priority while aggregating and it has clearly be seen that similar domains are aggregated more than others

4 Result and Discussion

We conduct experiments under both IID and Non-IID settings. Non-IID scenarios are simulated using Dirichlet sampling with concentration parameter $\alpha \in \{0.005, 0.01, 0.1\}$, where lower α induces higher class imbalance. For test-time adaptation, we evaluate Tent Wang et al. (2021a), CoTTA Wang et al. (2022), RoTTA Yuan et al. (2023), and ROID Marsden et al. (2024). In federated settings, we compare FedAvg McMahan et al. (2017), FedAvg-M Cheng et al. (2024), FedProx Li et al. (2020), pFedGraph Ye et al. (2023), and FedAMP Huang et al. (2021), with 10 simulated clients. Robustness under distribution shifts is assessed on CIFAR-10-C and CIFAR-100-C with 15 corruption types at severity level 5, using WideResNet-28 and ResNeXt-29, respectively.

4.1 Detailed Results

Table 1 presents a comprehensive performance comparison across various federated learning aggregation strategies and test-time adaptation (TTA) methods, evaluated on two corruption-augmented benchmarks: CIFAR-10-C and CIFAR-100-C. The experiments are conducted in both IID and Non-IID client data settings, where Non-IID scenarios are simulated using Dirichlet distributions by varying the concentration parameter $\alpha \in \{0.005, 0.01, 0.1\}$. Lower values of α induce higher class imbalance across clients, thereby increasing the difficulty of the federated learning.

Performance under IID Setting. In the IID case, where data is evenly distributed across clients without class imbalance, most existing TTA methods such as Tent, CoTTA, and ROID demonstrate strong performance when paired with standard federated aggregation techniques like FedAvg and FedProx. For instance, Tent and CoTTA achieve over 81% accuracy on CIFAR-10-C across multiple aggregation strategies. Our proposed BBN method remains competitive, achieving consistent performance over 70% and 59% on the CIFAR-10-C and CIFAR-100-C datasets respectively.

Performance under Non-IID Setting. Under the more realistic Non-IID setting with varying degrees of class imbalance (controlled by Dirichlet α), the performance of standard TTA methods degrades significantly. In particular, methods like Tent and CoTTA drop to as low as 6–30% accuracy in extreme imbalance cases ($\alpha = 0.005$) across both datasets. In contrast, our proposed TTA method BBN maintains robust performance across all levels of imbalance. For example, with FedAvg at $\alpha = 0.005$, BBN achieves 68.47% on CIFAR-10-C and 67.49% on CIFAR-100-C, substantially outperforming other methods.

Superior Performance of pFedBBN. Notably, our full framework, pFedBBN, which combines personalized federated learning with the BBN-based TTA strategy, consistently achieves the highest or near-highest accuracy across all scenarios. It maintains stable performance even in highly imbalanced cases. For instance, on CIFAR-10-C with $\alpha = 0.005$, pFedBBN achieves 72.41%, surpassing all other combinations of FL and TTA strategies. Similarly, on CIFAR-100-C, it reaches 73.88%

accuracy at $\alpha = 0.01$, demonstrating both robustness and effectiveness in diverse settings. These results show that while existing TTA methods falter under class imbalance and data heterogeneity, our BBN-based TTA, especially with pFedBBN, offers a more effective solution.

Comparison of TTA setups under heterogeneity. In Fig. 2a and Fig. 2b respectively, we show the performances on CIFAR-10-C and CIFAR-100-C datasets respectively for various test time adaptation techniques. For, CIFAR-10-C, provides almost consistent performance under all fed setups, while RoTTA falls slightly short. Our method is comparable to the techniques, and beats both the aforementioned techniques for pFedGraph aggregation. In Fig. 2b for the evaluation of CIFAR-100-C corruption dataset, our method consistently outperforms all the TTA methods under all aggregation setups. These results demonstrate BBN's robustness under various domain shifts.

Performance analysis under domain shift In Fig. 3 we demonstrate BBN's performance across different domains under class imbalance (α) = 0.01 for various aggregation techniques. We observe that for FedAvg aggregation our method performs the best across a diversity of corruption settings. This indicates better generalization under FedAvg aggregation. The personalized setup, pFedGraph comes in second with competitive performance for various corruptions eg: Gaussian Noise, Shot Noise, Fog, Brightness, JPEG compression, etc. From the figure, it is also evident that our method performs best in lighting and weather corruptions, modestly on noise corruptions, but struggles with blur, compression, and geometric distortions.

Performance analysis of Major and Minor Classes of pFedBBN As shown in Fig. 4, pFedBBN consistently achieves strong performance across all clients, maintaining at least 50% accuracy in both major and minor classes. However in Fig. 5, in the case of clients 2 and 8, we observe noticeable drops in accuracy under certain domain shifts. This indicates the presence of significant distribution shifts as these clients transition across domains, highlighting the challenges posed by continual domain adaptation.

Collaboration Weight Analysis of Client Aggregation in pFedBBN We compute a symmetric distance matrix based on the Balanced Batch Normalization (BBN) statistics, specifically, the global mean and variance, across all clients. This matrix is then used to derive the collaboration weights for aggregation. The results reveal that clients tend to prioritize aggregation with others from the same domain, highlighting domain-aware collaboration. As shown in Fig. 6, clients from similar domains consistently form clusters in the collaboration weight matrix across different federated rounds, indicating effective domain-wise distribution alignment.

5 Conclusion

We introduced **pFedBBN**, a federated test-time adaptation framework that addresses class imbalance and domain shifts by leveraging Balanced Batch Normalization. FedBBN enables unsupervised, privacy-preserving client-side adaptation and introduces a class-aware server aggregation strategy. Experiments on benchmark datasets show that FedBBN improves robustness and minority-class performance over existing methods. This makes it a practical and scalable solution for real-world federated learning scenarios with non-IID and unlabeled test distributions.

References

Chuan Chen, Tianchi Liao, Xiaojun Deng, Zihou Wu, Sheng Huang, and Zibin Zheng. Advances in robust federated learning: A survey with heterogeneity considerations. *IEEE Transactions on Big Data*, 2025.

Ziheng Cheng, Xinmeng Huang, Pengfei Wu, and Kun Yuan. Momentum benefits non-iid federated learning simply and provably. In *The Twelfth International Conference on Learning Representations*, 2024. URL https://openreview.net/forum?id=TdhkAcXkRi.

Moming Duan, Duo Liu, Xianzhang Chen, Renping Liu, Yujuan Tan, and Liang Liang. Self-balancing federated learning with global imbalanced data in mobile systems. *IEEE Transactions on Parallel and Distributed Systems*, 32(1):59–71, 2020.

Chen Huang, Yining Li, Chen Change Loy, and Xiaoou Tang. Learning deep representation for imbalanced classification. In *Proceedings of the IEEE conference on computer vision and pattern recognition*, pp. 5375–5384, 2016.

Yutao Huang, Lingyang Chu, Zirui Zhou, Lanjun Wang, Jiangchuan Liu, Jian Pei, and Yong Zhang. Personalized cross-silo federated learning on non-iid data. *Proceedings of the AAAI Conference on Artificial Intelligence*, 35(9):7865–7873, May 2021. doi: 10.1609/aaai.v35i9.16960. URL https://ojs.aaai.org/index.php/AAAI/article/view/16960.

Salman H Khan, Munawar Hayat, Mohammed Bennamoun, Ferdous A Sohel, and Roberto Togneri. Cost-sensitive learning of deep feature representations from imbalanced data. *IEEE transactions on neural networks and learning systems*, 29(8):3573–3587, 2017.

Matloob Khushi, Kamran Shaukat, Talha Mahboob Alam, Ibrahim A Hameed, Shahadat Uddin, Suhuai Luo, Xiaoyan Yang, and Maranatha Consuelo Reyes. A comparative performance analysis of data resampling methods on imbalance medical data. *Ieee Access*, 9:109960–109975, 2021.

Tian Li, Anit Kumar Sahu, Manzil Zaheer, Maziar Sanjabi, Ameet Talwalkar, and Virginia Smith. Federated optimization in heterogeneous networks. *Proceedings of Machine learning and systems*, 2:429–450, 2020.

Bingyan Liu, Nuoyan Lv, Yuanchun Guo, and Yawen Li. Recent advances on federated learning: A systematic survey. *Neurocomputing*, 597:128019, 2024.

Robert A Marsden, Mario Döbler, and Bin Yang. Universal test-time adaptation through weight ensembling, diversity weighting, and prior correction. In *Proceedings of the IEEE/CVF Winter Conference on Applications of Computer Vision*, pp. 2555–2565, 2024.

Brendan McMahan, Eider Moore, Daniel Ramage, Seth Hampson, and Blaise Aguera y Arcas. Communication-efficient learning of deep networks from decentralized data. In *Artificial intelligence and statistics*, pp. 1273–1282. PMLR, 2017.

Shuaicheng Niu, Jiaxiang Wu, Yifan Zhang, Yaofo Chen, Shijian Zheng, Peilin Zhao, and Mingkui Tan. Efficient test-time model adaptation without forgetting. In *Proceedings of the 39th International Conference on Machine Learning (ICML)*, volume 162 of *Proceedings of Machine Learning Research*, pp. 16888–16905. PMLR, 17–23 Jul 2022.

Maxence Noble, Aurélien Bellet, and Aymeric Dieuleveut. Differentially private federated learning on heterogeneous data. In *International conference on artificial intelligence and statistics*, pp. 10110–10145. PMLR, 2022.

Rakibul Hasan Rajib, Md Akil Raihan Iftee, Mir Sazzat Hossain, AKM Rahman, Sajib Mistry, M Ashraful Amin, and Amin Ahsan Ali. Fedctta: A collaborative approach to continual test-time adaptation in federated learning. *arXiv preprint arXiv:2505.13643*, 2025.

Dipankar Sarkar, Ankur Narang, and Sumit Rai. Fed-focal loss for imbalanced data classification in federated learning. *arXiv preprint arXiv:2011.06283*, 2020.

Mihye Seol and Taejoon Kim. Performance enhancement in federated learning by reducing class imbalance of non-iid data. *Sensors*, 23(3):1152, 2023.

Dequan Wang, Evan Shelhamer, Shaoteng Liu, Bruno Olshausen, and Trevor Darrell. Tent: Fully test-time adaptation by entropy minimization. In *International Conference on Learning Representations*, 2021a. URL https://arxiv.org/abs/2006.10726.

Lixu Wang, Shichao Xu, Xiao Wang, and Qi Zhu. Addressing class imbalance in federated learning. In *Proceedings of the AAAI conference on artificial intelligence*, volume 35, pp. 10165–10173, 2021b.

Qin Wang, Olga Fink, Luc Van Gool, and Dengxin Dai. Continual test-time domain adaptation. In *Proceedings of the IEEE/CVF Conference on Computer Vision and Pattern Recognition*, pp. 7201–7211, 2022.

Yu-Xiong Wang, Deva Ramanan, and Martial Hebert. Learning to model the tail. *Advances in neural information processing systems*, 30, 2017.

Chenguang Xiao and Shuo Wang. An experimental study of class imbalance in federated learning. In *2021 IEEE Symposium Series on Computational Intelligence (SSCI)*, pp. 1–7. IEEE, 2021.

Rui Ye, Zhenyang Ni, Fangzhao Wu, Siheng Chen, and Yanfeng Wang. Personalized federated learning with inferred collaboration graphs. In *International conference on machine learning*, pp. 39801–39817. PMLR, 2023.

Fuming You, Jingjing Li, and Zhou Zhao. Test-time batch statistics calibration for covariate shift. *arXiv preprint arXiv:2110.04065*, 2021.

Longhui Yuan, Binhui Xie, and Shuang Li. Robust test-time adaptation in dynamic scenarios. In *Proceedings of the IEEE/CVF Conference on Computer Vision and Pattern Recognition*, pp. 15922–15932, 2023.

A Appendix

B Dataset Details

We evaluate our methods on the CIFAR-10-C and CIFAR-100-C benchmarks, which apply 15 common image corruptions (e.g., Gaussian noise, blur, brightness) at five discrete severity levels $\{1, \ldots, 5\}$. The original CIFAR-10 and CIFAR-100 test sets each contain 10,000 images. For each of the 15 corruption types, the corrupted dataset contains 50,000 images (10,000 images per severity level, across five levels). The total benchmark for a dataset, like CIFAR-10-C, therefore contains 750,000 images, which are grouped into 10 and 100 classes respectively. In this work, we focus exclusively on the worst-case noise level: severity-5. Therefore, in our work, we simulate maximal domain shift and stress-test the model's robustness.

C Personalized Federated Balanced Batch Normalization

The pFedBBN algorithm is a personalized federated learning setup designed to tackle the data heterogeneity and class imbalance problem in test-time adaptation (TTA). This method focuses on Batch normalization statistics and a unique aggregation strategy. The process begins with the server broadcasting the current global model to all participating clients. Each client then independently performs a balanced batch normalization in test time adaptation on its local, unlabeled test data. This client-side adaptation is crucial as it not only fine-tunes the model to the client's specific data distribution but also addresses class imbalance by using a balanced loss function and pseudo label generated at test time as ground truth is not available. After local adaptation, each client extracts and sends its Batch Normalization (BN) statistics (mean and variance for each layer) back to the server. The server, instead of a simply averaging, uses the collected BN statistics to compute a collaboration matrix. This matrix quantifies the similarity between the data distributions of different clients, effectively utilizing the information of relatedness among the clients. A higher similarity between two clients' BN statistics results in a stronger collaboration weight. The server uses this collaboration matrix to perform a weighted aggregation, creating a personalized aggregated model for each client. This approach ensures that clients with similar data distributions contribute more to each other's model updates. This iterative process allows the global model to converge while maintaining the personalized characteristics of each client's model, making it robust to non-IID data.

C.1 Code Appendix

C.1.1 Command-Line Usage

To reproduce experiments on CIFAR-10-C (Dirichlet $\alpha = 0.005$) with BBN-TTA and pFedBBN:

```
python test_time_new.py \
  --cfg cfgs/cifar10_c/bbn_tta.yaml \
```

Pseudocode 1 pFedBBN: Personalized Federated BN-Statistics Aggregation

K clients, each with local BN statistics $B_i = \{(\mu_\ell^i, \sigma_\ell^{2,i})\}_{\ell=1}^L$; temperature T each communication round Clients $1 \dots K$ send B_i to server Server computes distances: $D_{ij} = \frac{1}{L}\sum_{\ell=1}^L (\|\mu_\ell^i - \mu_\ell^j\| + \|\sigma_\ell^{2,i} - \sigma_\ell^{2,j}\|)$ Compute weights: $W_{i\to j} = \exp(-D_{ij}/T)$ and row-normalize each client i Aggregate: $\theta_i \leftarrow \sum_{j=1}^K W_{i\to j}\,\theta_j$ Server broadcasts updated $\{\theta_i\}$ back to clients

```
fed.fed_tech fedbnstat \
fed.dirichlet_alpha 0.005
```

C.1.2 Code Structure and Notes

- **test_time_new.py**: main entry point—parses flags, loads config, dispatches to BBN-TTA or other TTA.
- **bbn_tta.py**: implements BBN-TTA adaptation (BN-affine updates, pseudo-labeling, entropy mask).
- **fedbnstat_group.py**: server-side logic for BN stat collection, distance computation, weight normalization, model aggregation.
- **Hyperparameters**: defined in `conf.py` (e.g., H_0, λ, learning rates, batch size).
- **Environment**: NVIDIA A100 GPUs, PyTorch 1.13, CUDA 11.7, Ubuntu 20.04.

D Additional Analysis

D.1 Performance Gain of pFedBBN over Baselines

We illustrate the performance gain of our proposed pFedBBN method over several standard and advanced federated learning baselines across figure 7 to figure 9, all of which are combined with our client-side BBN TTA. These figures provide a clear visual comparison of how our novel BN statistics aggregation strategy, a core component of pFedBBN, improves upon existing federated methods. Specifically, Figure 7 compares pFedBBN against the FedAvg baseline, Figure 8 highlights the improvements against the personalized graph-based pFedGraph, and Figure 10 demonstrates the gain over the personalized FedAmp method. The consistent positive accuracy gains across various non-IID degrees on both CIFAR-10-C and CIFAR-100-C datasets serve as strong evidence that our aggregation approach is more effective at leveraging BN statistics for robust, personalized model updates.

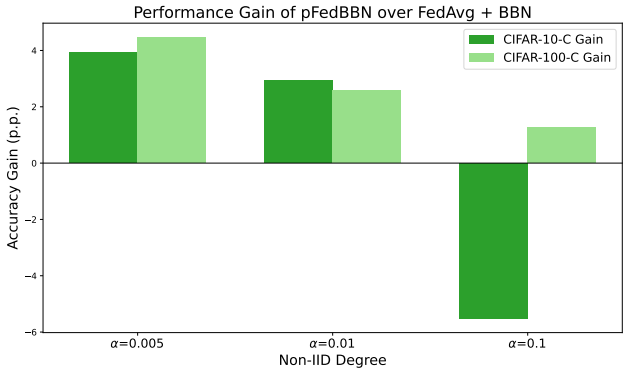

Figure 7: pFedBBN gain over FedAvgBBN.

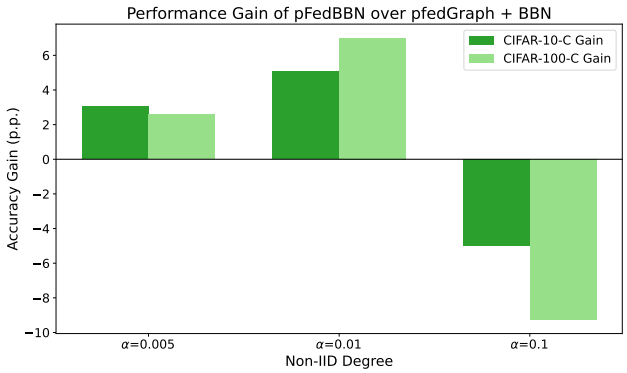

Figure 8: pFedBBN gain over pFedGraphBBN.

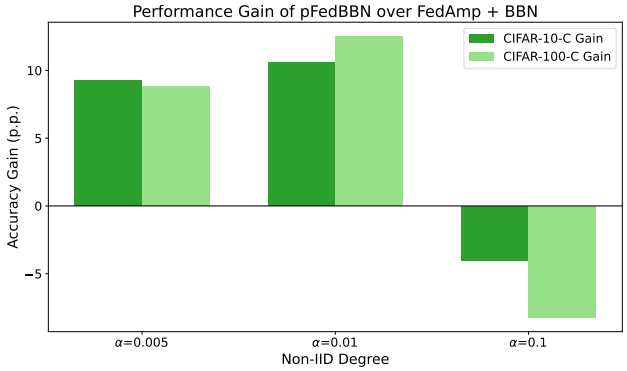

Figure 9: pFedBBN gain over FedAMPBBN.

D.2 Class imbalance analysis

Figure 10 and Figure 11 provide a detailed analysis of the simulated class imbalance, which is crucial for understanding the challenges of the non-IID setting. Figure 10, the Global Class Frequency plot, visually represents the severe class imbalance inherent in the CIFAR-10-C data distribution with a Dirichlet α of 0.005. It highlights the long-tail problem where a small number of classes dominate the dataset, while others are significantly under-represented. This imbalance is a primary driver of poor model performance in federated learning. Figure 11, the Global Normalized Imbalance Over Time plot, offers an insightful look into the training dynamics. This line graph tracks the normalized imbalance across federated rounds, showing how the model, despite the initial data disparity, learns to progressively correct for the imbalance. This demonstrates the effectiveness of the training process in mitigating dataset heterogeneity, a key objective of our method.

D.3 Performance comparison of Fed TTA setups

A performance comparison across federated methods and Test-Time Adaptation (TTA) strategies is presented in Figures 12 through 17. A key observation across all scenarios is the distinct performance clusters formed by the TTA methods. Figures 12, 13, and 14 show that on the CIFAR-10-C dataset, TTA methods like Tent, CoTTA, and ROID consistently underperform, with accuracy scores generally below 30%. In stark contrast, RoTTA and BBN achieve significantly higher accuracies, often exceeding 60% and 70% respectively, making them the superior choices for TTA. This trend is echoed in the CIFAR-100-C results, as shown in Figures 15, 16, and 17, where Tent, CoTTA, and ROID again exhibit very low accuracy, sometimes in the single digits, while RoTTA and BBN maintain high performance levels. Notably, the federated methods—FedAvg, pfedGraph, and FedAmp—show comparable performance with a given TTA method. However, the BBN TTA method paired with these federated methods generally yields the highest overall accuracy.

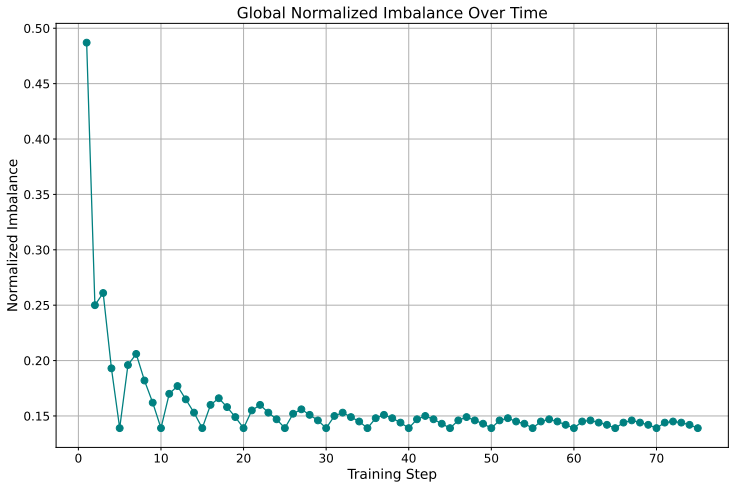

Figure 10: Global imbalance ratio with federated rounds.

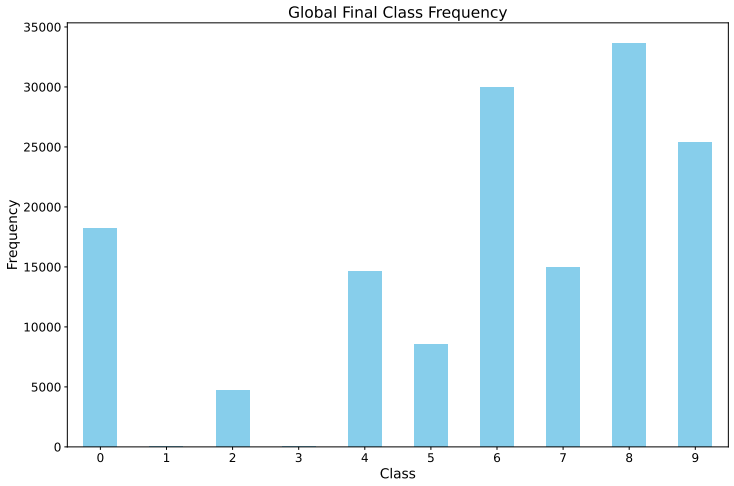

Figure 11: Global class frequency for CIFAR-10-C.

D.4 IID ANALYSIS

In Figures 18 and 19, we provide a foundational analysis of model performance under IID (Independent and Identically Distributed) conditions, a crucial baseline for evaluating federated learning methods. The plots for CIFAR-10-C and CIFAR-100-C respectively, demonstrate that when data is evenly distributed across clients, all federated methods—both with and without TTA (Test-Time Adaptation) methods like BBN—achieve high and comparable accuracy. The lack of significant performance gaps in this setting confirms that the primary challenge of federated learning is not the distributed nature of the data itself, but rather the data heterogeneity introduced by non-IID distributions.

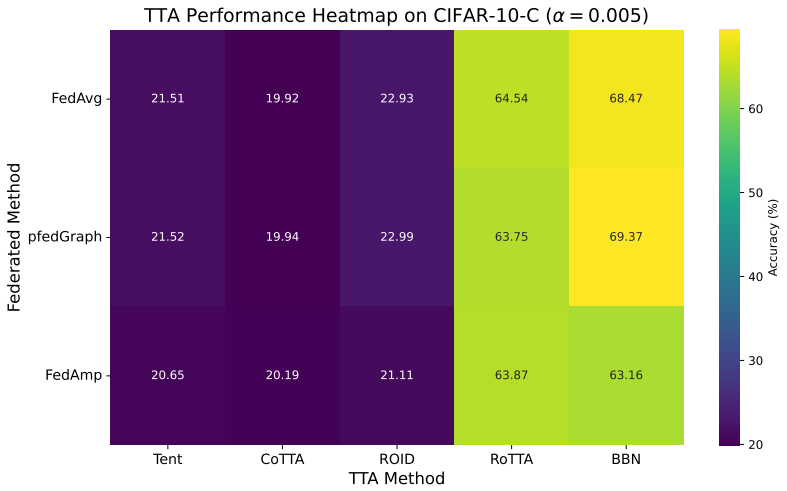

Figure 12: Fed TTA performance on CIFAR-10-C ($\alpha = 0.005$)

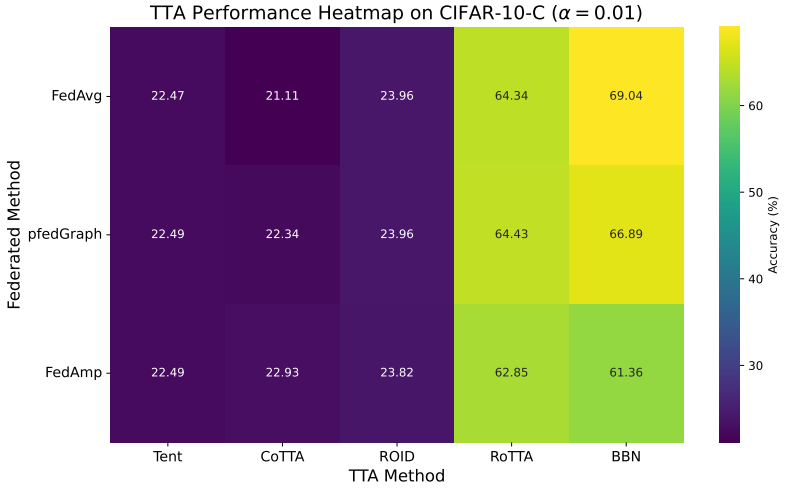

Figure 13: Fed TTA performance on CIFAR-10-C ($\alpha = 0.01$)

Table 2: Average global class accuracy (%) on CIFAR-10-C and CIFAR-100-C under Dirichlet heterogeneity $\alpha = 0.01$. Results are grouped by dataset and TTA method, then compared across four federated aggregation schemes (None-Fed, FedAvg, pFedGraph, FedAMP) plus the "centralized" CoTTA baseline. Higher values indicate better robustness to distribution skew.

Dataset	TTA Method	Federated Algorithm				
		None-Fed	FedAvg	pFedGraph	FedAmp	CoTTA
CIFAR-10-C	Tent	23.9	29.12	29.14	29.05	28.0
	CoTTA	25.5	30.0	30.1	30.0	30.0
	ROID	22.0	30.64	30.64	30.52	29.5
	RoTTA	36.42	59.37	59.46	58.33	57.0
	BBN	52.43	62.24	61.14	58.22	59.0
CIFAR-100-C	Tent	10.3	12.73	12.71	13.04	13.0
	CoTTA	12.0	14.5	14.7	14.6	14.6
	ROID	12.0	15.56	15.49	15.54	15.0
	RoTTA	17.31	25.11	25.19	24.97	24.0
	BBN	29.65	29.92	30.13	30.25	30.0

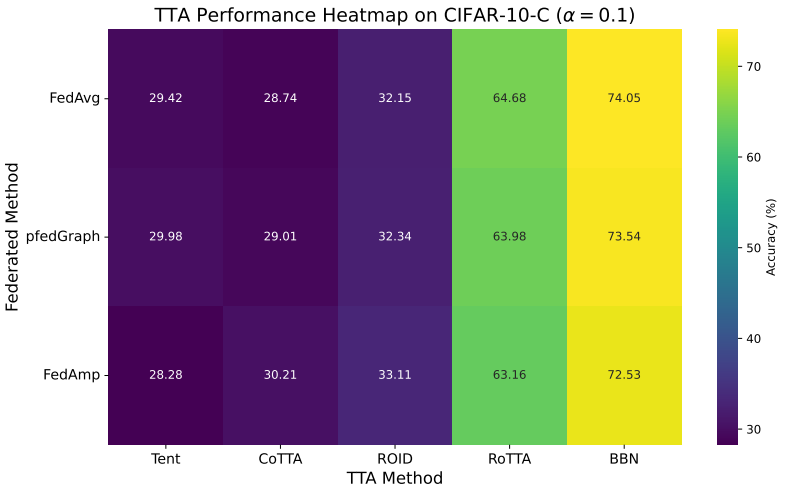

Figure 14: Fed TTA performance on CIFAR-10-C ($\alpha = 0.1$)

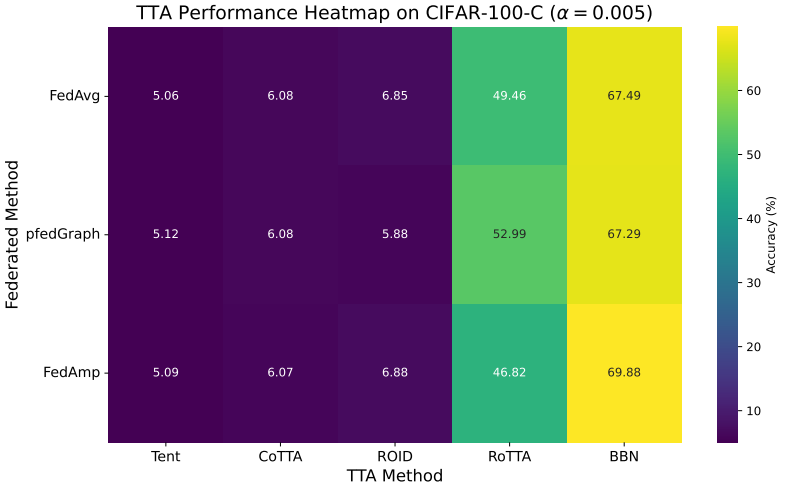

Figure 15: Fed TTA performance on CIFAR-100-C ($\alpha = 0.005$)

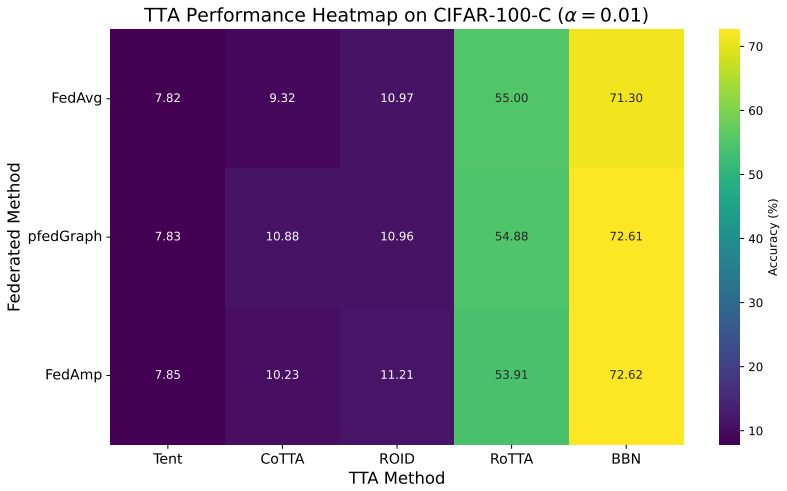

Figure 16: Fed TTA performance on CIFAR-100-C ($\alpha = 0.01$)

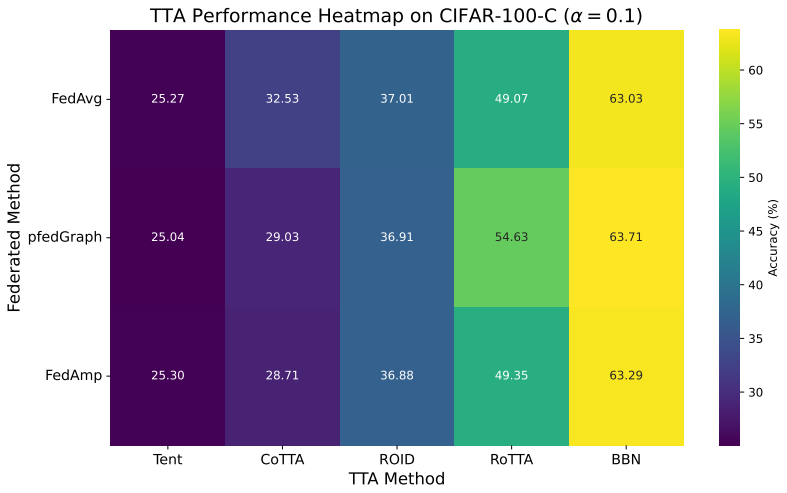

Figure 17: Fed TTA performance on CIFAR-100-C ($\alpha = 0.1$)

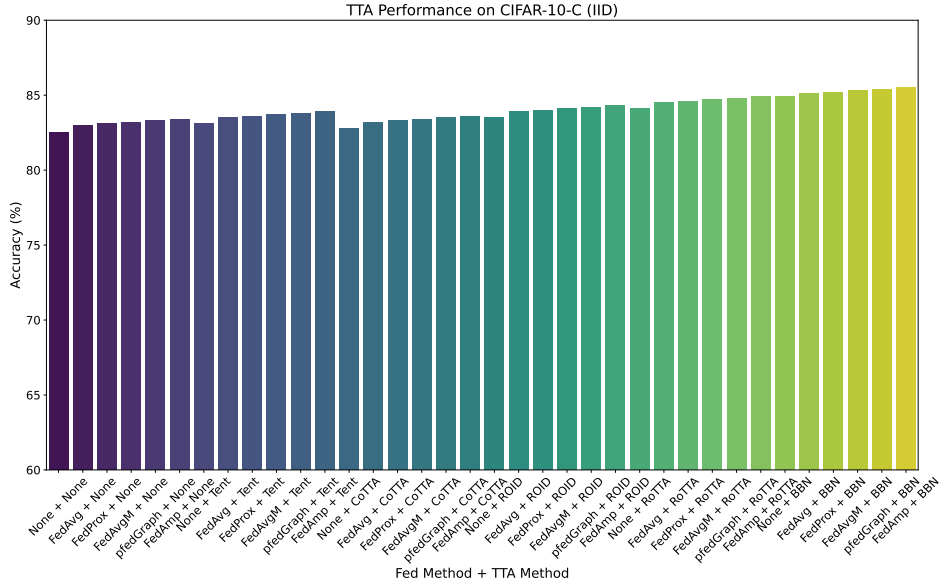

Figure 18: CIFAR-10-C IID performance.

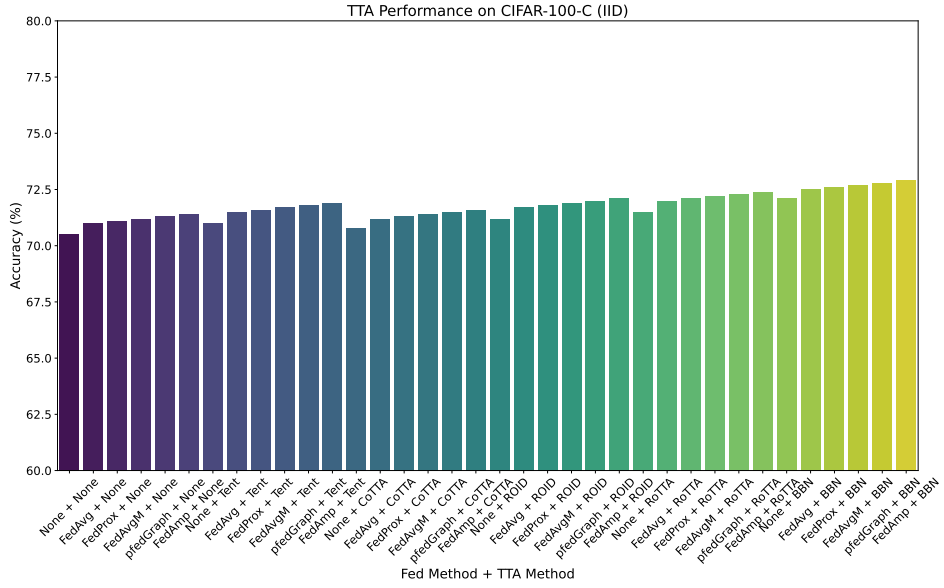

Figure 19: CIFAR-100-C IID performance.

Table 3: Class-wise global accuracy (%) on CIFAR-10-C (severity-5) under Dirichlet heterogeneity $\alpha = 0.01$. We compare four TTA methods (Tent, CoTTA, ROID, RoTTA, BBN) across four federation schemes (None, FedAvg, pFedGraph, FedAMP). The low α simulates extreme non-IID (no client observes class 3), so class 3 accuracy is zero across all settings.

Method	Fed	C0	C1	C2	C3	C4	C5	C6	C7	C8	C9	Avg
Tent	None-Fed	21.5	67.5	30.0	0.0	35.0	42.0	20.0	45.0	34.0	44.0	33.9
Tent	FedAvg	28.0	82.0	50.0	0.0	56.0	62.0	65.0	74.0	62.0	80.0	55.9
Tent	pFedGraph	28.3	81.8	49.5	0.0	56.5	61.8	61.5	73.0	60.5	79.2	55.3
Tent	FedAMP	27.8	81.0	48.5	0.0	55.0	61.2	58.0	72.5	58.5	78.0	54.0
CoTTA	None-Fed	23.0	68.0	32.0	0.0	36.5	43.0	22.0	47.0	35.5	46.0	35.0
CoTTA	FedAvg	29.5	83.0	52.0	0.0	58.0	63.5	66.5	75.5	63.5	81.5	57.3
CoTTA	pFedGraph	29.7	82.9	51.5	0.0	58.4	63.1	63.1	74.2	62.0	80.6	56.6
CoTTA	FedAMP	29.1	82.5	50.5	0.0	57.1	62.7	60.2	73.5	60.2	79.5	55.6
ROID	None-Fed	19.0	62.0	28.0	0.0	32.0	39.0	18.0	42.0	31.0	42.0	31.3
ROID	FedAvg	30.6	81.4	54.0	0.0	59.0	65.0	67.0	76.5	65.0	83.0	58.2
ROID	pFedGraph	30.5	81.3	53.2	0.0	59.2	64.6	64.0	75.0	63.2	81.9	57.3
ROID	FedAMP	30.2	80.9	52.0	0.0	57.6	63.8	61.0	74.0	61.5	80.3	56.1
RoTTA	None-Fed	47.72	57.33	41.10	0.0	30.11	33.58	39.83	33.22	39.37	41.91	36.42
RoTTA	FedAvg	69.21	86.67	54.09	0.0	58.96	63.56	66.00	66.31	60.89	67.97	59.37
RoTTA	pFedGraph	69.76	85.33	53.25	0.0	59.25	65.89	63.94	67.29	61.73	68.13	59.46
RoTTA	FedAMP	66.36	84.00	54.16	0.0	57.35	64.83	61.41	67.20	59.60	68.43	58.33
BBN	None-Fed	47.33	84.00	51.46	0.0	55.97	68.61	36.86	64.67	47.85	67.57	52.43
BBN	FedAvg	63.48	85.33	50.96	0.0	57.20	67.80	70.10	79.15	66.23	82.17	62.24
BBN	pFedGraph	63.46	85.33	51.19	0.0	57.30	67.28	62.11	78.89	63.75	82.13	61.14
BBN	FedAMP	61.25	84.00	52.26	0.0	55.50	67.54	46.26	79.59	56.36	79.44	58.22

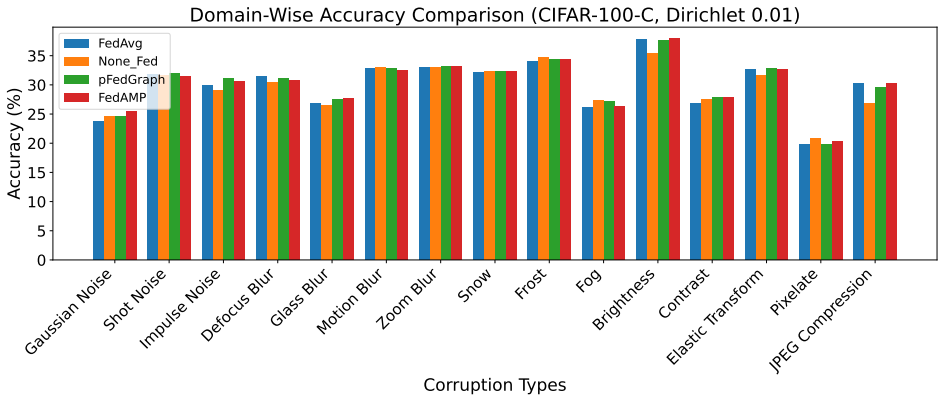

Figure 20: Domain-wise accuracy comparison of our method (Dirichlet α = 0.01) across CIFAR-100-C corruptions.

Table 4: Class-wise sample counts for CIFAR-10-C under Dirichlet heterogeneity $\alpha = 0.01$, rounds 1–45. Each row shows how many examples of each class a client sees in that test round, illustrating extreme non-IID splits (e.g., class 3 never appears).

Round	Class 0	Class 1	Class 2	Class 3	Class 4	Class 5	Class 6	Class 7	Class 8	Class 9
1	496	5	268	0	200	0	327	200	304	200
2	266	0	199	0	202	132	400	200	401	200
3	200	0	0	0	200	200	400	200	400	400
4	200	0	0	0	200	115	400	200	485	400
5	200	0	0	0	53	10	400	200	736	401
6	496	5	268	0	200	0	327	200	304	200
7	266	0	199	0	202	132	400	200	401	200
8	200	0	0	0	200	200	400	200	400	400
9	200	0	0	0	200	115	400	200	485	400
10	200	0	0	0	53	10	400	200	736	401
11	496	5	268	0	200	0	327	200	304	200
12	266	0	199	0	202	132	400	200	401	200
13	200	0	0	0	200	200	400	200	400	400
14	200	0	0	0	200	115	400	200	485	400
15	200	0	0	0	53	10	400	200	736	401
16	496	5	268	0	200	0	327	200	304	200
17	266	0	199	0	202	132	400	200	401	200
18	200	0	0	0	200	200	400	200	400	400
19	200	0	0	0	200	115	400	200	485	400
20	200	0	0	0	53	10	400	200	736	401
21	496	5	268	0	200	0	327	200	304	200
22	266	0	199	0	202	132	400	200	401	200
23	200	0	0	0	200	200	400	200	400	400
24	200	0	0	0	200	115	400	200	485	400
25	200	0	0	0	53	10	400	200	736	401
26	496	5	268	0	200	0	327	200	304	200
27	266	0	199	0	202	132	400	200	401	200
28	200	0	0	0	200	200	400	200	400	400
29	200	0	0	0	200	115	400	200	485	400
30	200	0	0	0	53	10	400	200	736	401
31	496	5	268	0	200	0	327	200	304	200
32	266	0	199	0	202	132	400	200	401	200
33	200	0	0	0	200	200	400	200	400	400
34	200	0	0	0	200	115	400	200	485	400
35	200	0	0	0	53	10	400	200	736	401
36	496	5	268	0	200	0	327	200	304	200
37	266	0	199	0	202	132	400	200	401	200
38	200	0	0	0	200	200	400	200	400	400
39	200	0	0	0	200	115	400	200	485	400
40	200	0	0	0	53	10	400	200	736	401
41	496	5	268	0	200	0	327	200	304	200
42	266	0	199	0	202	132	400	200	401	200
43	200	0	0	0	200	200	400	200	400	400
44	200	0	0	0	200	115	400	200	485	400
45	200	0	0	0	53	10	400	200	736	401

Table 5: Class-wise sample counts for CIFAR-10-C under Dirichlet heterogeneity $\alpha = 0.01$, rounds 46–75. Each row shows how many examples of each class a client sees in that test round, illustrating extreme non-IID splits (e.g., class 3 never appears).

Round	Class 0	Class 1	Class 2	Class 3	Class 4	Class 5	Class 6	Class 7	Class 8	Class 9
46	496	5	268	0	200	0	327	200	304	200
47	266	0	199	0	202	132	400	200	401	200
48	200	0	0	0	200	200	400	200	400	400
49	200	0	0	0	200	115	400	200	485	400
50	200	0	0	0	53	10	400	200	736	401
51	496	5	268	0	200	0	327	200	304	200
52	266	0	199	0	202	132	400	200	401	200
53	200	0	0	0	200	200	400	200	400	400
54	200	0	0	0	200	115	400	200	485	400
55	200	0	0	0	53	10	400	200	736	401
56	496	5	268	0	200	0	327	200	304	200
57	266	0	199	0	202	132	400	200	401	200
58	200	0	0	0	200	200	400	200	400	400
59	200	0	0	0	200	115	400	200	485	400
60	200	0	0	0	53	10	400	200	736	401
61	496	5	268	0	200	0	327	200	304	200
62	266	0	199	0	202	132	400	200	401	200
63	200	0	0	0	200	200	400	200	400	400
64	200	0	0	0	200	115	400	200	485	400
65	200	0	0	0	53	10	400	200	736	401
66	496	5	268	0	200	0	327	200	304	200
67	266	0	199	0	202	132	400	200	401	200
68	200	0	0	0	200	200	400	200	400	400
69	200	0	0	0	200	115	400	200	485	400
70	200	0	0	0	53	10	400	200	736	401
71	496	5	268	0	200	0	327	200	304	200
72	266	0	199	0	202	132	400	200	401	200
73	200	0	0	0	200	200	400	200	400	400
74	200	0	0	0	200	115	400	200	485	400
75	200	0	0	0	53	10	400	200	736	401

Table 6: Domain-wise average accuracy (%) on CIFAR-10-C (severity-5) under Dirichlet heterogeneity $\alpha = 0.01$, comparing five TTA methods (TENT, CoTTA, ROID, RoTTA, BBN) across four federation schemes: FedAvg, None-Fed, pFedGraph, and FedAMP. Each block of five columns corresponds to one federation strategy, with "None-Fed" values indicating no federated strategy. The accuracy values under 15 corruption types are shown in the table.

Corruption	**FedAvg**					**None-Fed**				
	Tent	CoTTA	ROID	RoTTA	BBN	Tent	CoTTA	ROID	RoTTA	BBN
Gaussian Noise	27.61	38.48	29.54	49.35	50.81	27.60	32.90	29.53	38.21	48.39
Shot Noise	27.93	43.30	29.57	58.66	64.45	27.86	36.98	29.60	32.25	56.37
Impulse Noise	25.49	36.81	26.60	48.14	51.47	25.46	33.53	26.61	41.64	37.20
Defocus Blur	30.88	40.44	33.11	49.99	50.70	30.82	40.44	33.08	14.10	38.01
Glass Blur	24.02	39.19	25.10	54.35	56.74	24.01	30.82	25.16	37.63	36.58
Motion Blur	30.92	46.89	32.67	62.86	66.80	30.92	40.37	32.69	33.85	51.72
Zoom Blur	30.76	46.89	33.04	63.01	70.50	30.68	46.89	33.02	65.85	59.04
Snow	29.75	50.29	31.35	72.82	68.50	29.76	51.16	31.36	48.01	58.49
Frost	30.55	53.32	32.10	76.09	76.74	30.54	47.54	32.08	50.95	68.36
Fog	31.30	49.44	33.01	67.57	73.26	31.29	49.44	32.98	52.19	60.41
Brightness	32.54	56.46	34.25	81.75	81.17	32.43	56.03	34.28	46.79	74.21
Contrast	31.18	39.17	32.82	47.16	49.33	31.10	36.03	32.83	9.07	41.22
Elastic Transform	28.05	42.33	28.76	56.61	61.05	28.05	36.57	28.76	17.90	52.74
Pixelate	28.97	36.65	30.22	44.33	50.08	28.97	40.20	30.19	33.02	47.09
JPEG Compression	26.89	39.17	27.45	57.82	62.05	26.90	33.90	27.46	24.82	56.64

Corruption	**pFedGraph**					**FedAMP**				
	Tent	CoTTA	ROID	RoTTA	BBN	Tent	CoTTA	ROID	RoTTA	BBN
Gaussian Noise	50.81	39.21	29.52	50.81	52.58	50.75	39.21	29.48	50.75	52.35
Shot Noise	59.36	43.64	29.59	59.36	64.08	60.88	44.41	29.54	60.88	61.31
Impulse Noise	49.04	37.27	26.62	49.04	52.84	50.59	38.05	26.49	50.59	51.98
Defocus Blur	49.97	40.42	33.11	49.97	47.74	44.32	37.63	32.92	44.32	44.75
Glass Blur	54.27	39.15	25.10	54.27	54.30	54.23	39.12	24.96	54.23	48.67
Motion Blur	62.99	46.95	32.74	62.99	64.46	60.95	45.95	32.60	60.95	58.09
Zoom Blur	62.88	46.92	33.04	62.88	68.93	63.27	46.86	32.95	63.27	66.86
Snow	72.95	50.36	31.37	72.95	66.66	70.67	48.05	31.19	70.67	64.76
Frost	76.10	53.35	32.05	76.10	76.49	74.63	52.04	31.92	74.63	73.62
Fog	67.55	49.43	33.00	67.55	70.61	64.76	44.66	32.88	64.76	68.73
Brightness	81.77	56.49	34.21	81.77	80.76	81.02	53.95	34.10	81.02	77.39
Contrast	47.40	39.22	32.86	47.40	47.40	39.90	39.21	32.72	39.90	45.21
Elastic Transform	56.39	35.52	28.75	56.39	59.69	55.67	36.88	28.58	55.67	53.76
Pixelate	42.07	42.61	30.17	42.07	49.52	44.79	42.74	30.14	44.79	48.36
JPEG Compression	58.32	39.29	27.48	58.32	61.09	58.56	42.74	27.38	58.56	57.48

Table 7: Client-wise accuracy (%) on CIFAR-10-C under Dirichlet $\alpha = 0.01$ Accuracy is reported for each client (0–9) using five TTA methods (Tent, CoTTA, ROID, RoTTA, BBN) across four federated learning setups: FedAvg, pFedGraph, FedAMP, and None-Fed. The bottom row shows the average accuracy across clients, highlighting the impact of personalization under non-IID settings.

Client	**FedAvg**					**None-Fed**				
	Tent	CoTTA	ROID	RoTTA	BBN	Tent	CoTTA	ROID	RoTTA	BBN
0	18.40	22.74	18.79	27.08	28.08	18.06	17.57	18.95	16.66	17.66
1	2.02	4.32	2.02	6.62	7.62	2.02	4.32	2.03	4.07	5.07
2	2.03	4.55	2.10	7.07	8.07	2.02	4.55	2.13	4.91	5.91
3	13.19	16.58	13.82	19.97	20.97	13.13	16.05	13.83	10.77	11.77
4	5.41	8.88	5.62	12.36	13.36	5.38	8.88	5.72	8.42	9.42
5	17.28	19.11	17.69	20.94	21.94	17.33	19.11	17.72	13.86	14.86
6	13.57	15.75	14.06	16.43	17.43	13.53	15.75	14.02	11.66	12.66
7	2.02	4.13	2.31	6.23	7.23	2.00	4.13	2.32	4.16	5.16
8	10.41	12.31	10.46	14.16	15.16	10.41	12.31	11.18	7.77	8.77
9	2.29	4.46	2.59	6.63	7.63	2.27	4.46	2.56	3.32	4.32
Mean	8.66	11.21	8.95	13.75	14.75	8.61	11.21	9.05	8.56	9.56
Client	**pFedGraph**					**FedAMP**				
	Tent	CoTTA	ROID	RoTTA	BBN	Tent	CoTTA	ROID	RoTTA	BBN
0	18.40	22.74	18.79	27.45	28.45	18.40	22.74	18.76	27.09	28.09
1	2.02	4.32	2.02	6.38	7.38	2.02	4.32	2.00	6.15	7.15
2	2.03	4.55	2.10	7.14	8.14	2.03	4.55	2.08	6.78	7.78
3	13.19	16.58	13.83	20.10	21.10	13.19	16.58	13.81	20.14	21.14
4	5.41	8.88	5.61	12.44	13.44	5.41	8.88	5.59	11.65	12.65
5	17.28	19.11	17.69	20.56	21.56	17.29	19.11	17.69	20.30	21.30
6	13.57	15.75	14.06	16.97	17.97	13.57	15.75	14.04	16.31	17.31
7	2.02	4.13	2.31	6.28	7.28	2.03	4.13	2.29	6.38	7.38
8	10.41	12.31	10.45	14.27	15.27	10.41	12.31	10.44	14.16	15.16
9	2.29	4.46	2.60	6.73	7.73	2.29	4.46	2.59	6.72	7.72
Mean	8.66	11.21	8.95	13.83	14.83	8.66	11.21	8.93	13.57	14.57